Simulation of coherent interactions between Rydberg atoms

F. Robicheaux,[1,*] J. V. Hernández,[1] T. Topçu,[1] and L. D. Noordam[2]
[1]*Department of Physics, Auburn University, Alabama 36849-5311, USA*
[2]*FOM Institute for Atomic and Molecular Physics, Kruislaan 407, 1098 SJ Amsterdam, The Netherlands*
(Received 20 May 2004; published 8 October 2004)

The results of a theoretical investigation of the coherent interaction between many Rydberg atoms are reported. The atoms are assumed to move very little during the time range we investigate. We describe the basic interaction between atoms and show that (contrary to previous theoretical studies) the interaction between the atoms can be coherent. The band structure for a perfect lattice of atoms and the density of states for an amorphous distribution of atoms are presented. We also give results for when the atoms are roughly positioned in a lattice. Finally, we performed detailed calculations to understand when the Rydberg interactions are too strong for an essential states type of approximation. The relevance of our results to previous measurements in a Rydberg gas and to possible future experiments is discussed.

DOI: 10.1103/PhysRevA.70.042703 PACS number(s): 34.60.+z, 32.80.Rm, 32.80.Pj, 78.67.Bf

I. INTRODUCTION

There have been several experimental and theoretical investigations into the properties of a dense gas of Rydberg atoms; by a dense gas, we mean there is a sufficient density of Rydberg atoms for the interaction between them to be important or measurable. Broadly speaking, interesting phenomena arise from many-body effects or from two-body effects. In Rydberg gases, the many-body effects are achieved through the strong interaction between the highly excited atoms and the small energy separation between highly excited states. Typically, the interaction potential between atoms is through the dipole-dipole interaction and is roughly proportional to the square of the radius of the atoms divided by the cube of the distance between the atoms.

In Refs. [1–6], atoms are excited into Rydberg states chosen such that resonant energy transfer can occur; in this process an atom in state A and an atom in state B interact and convert $A \rightarrow C$ and $B \rightarrow D$ because the total energy is roughly conserved $E_A + E_B \simeq E_C + E_D$. Possible richness can arise from the fact that states C or D can then transfer to atoms of states A or B. For example, three atoms in state $|AAB\rangle$ (i.e., atoms 1 and 2 in state A and atom 3 in state B) can make the transitions $|AAB\rangle \rightarrow |CAD\rangle \rightarrow |ACD\rangle$. In the experiments, the atoms are cold and barely move during the interesting time period. Thus, the transitions are coherent and can proceed in both directions. A gas of Rydberg atoms with these resonant energy transfers has been shown to have spectral properties that differ from what would be expected from single-particle physics. Thus, some aspect of many-body physics is present.

The interaction between a pair of Rydberg atoms gives rise to long-range potentials which can be significant. In Ref. [7], the van der Waals Rydberg-Rydberg coupling was strong enough to significantly broaden the Rydberg lines. In Refs. [8–10], the long-range potential affects the motion of the atoms. Two Rydberg atoms can be made to have an attractive or repulsive potential; in the case of the attractive potential, the atoms can accelerate toward each other and collide. In Ref. [11], the long-range potentials of two np Rydberg atoms couple at very large distances to two-atom states with $(n-1)d, ns$ character which cannot be excited in the single-atom limit. However, the forbidden levels are accessed when the density of Rydberg atoms is high enough to give pairs within the critical distance. The strong interaction between Rydberg atoms has been used in proposals for fast quantum gates [12] and for a dipole blockade [13].

Lastly, the interaction between several Rydberg atoms has many features in common with using a sequence of metal nanoparticles as a waveguide (as an example, see Ref. [14] and Secs. III A and V below). In this system, there is an optically excited plasmon wave below the diffraction limit that travels along an array of metal nanoparticles. Much of the physics is reproduced through a simple point-dipole model.

We present the results of theoretical investigations of many-body processes in a Rydberg gas. As in Refs. [2–6], the atoms will hardly move over the important time. But, unlike previous work where the atoms are at random positions inside the gas, we imagine the atoms have been prepared to have spatial correlation. The simplest case we investigated is when the atoms are positioned to be exactly on a cubic lattice. While this situation will probably never be experimentally realized, it has several features that may be of interest. The band structure of a single p state in a matrix of s-state atoms has particle or hole properties depending on the polarization relative to the wave number. We also investigated the density of states for a random spatial distribution of Rydberg atoms where there is one p state in a matrix of s-state atoms.

Next, we investigated a model that could be experimentally observed with current technology. In this model, a Rydberg atom is randomly placed inside a small region, but the small regions are regularly spaced. Some of the atoms will start in state A and the others in state B. This situation is sketched in Fig. 1. Such an array can be achieved by starting with atoms prepared in an optical lattice. Or more simply, a laser can be split and focused into small regions of a gas so

*Electronic address: robicfj@auburn.edu

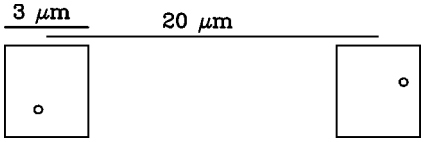

FIG. 1. Schematic drawing of a possible experiment to observe the coherent hopping of a Rydberg excitation. At $t=0$ an atom is excited into the highest energy $n=61$ state in an electric field in the leftmost region. In the right region, an atom is excited into the highest energy $n=60$ state. The $n=61$ state can hop to the atom in the right region. Which region contains the $n=60$ state can be determined by selective field ionization of the atoms onto a charge-coupled device (CCD) camera. The atoms have random positions within each region.

long as the width of a beam is smaller than the distance between the beams. For this case, we investigate the role that defects play in this system with special emphasis on changes that arise from no atom being present in a region or from two atoms being present in a small region.

In most discussions of Rydberg-Rydberg interactions, an essential states picture is used. In this picture, we include only the few states that are degenerate or nearly degenerate. This approximation should be accurate for many situations. However, we can expect the accuracy to decrease as the principal quantum number increases because the energy differences between states decreases as n increases. When n is high enough, a quasiclassical picture obtains and we should expect transitions between many states. Since most of our discussion will be based on the essential states model, it is important for us to understand the region where it is applicable. To address this, we directly solved the time-dependent Schrödinger equation within two simplified models.

Atomic units are used except where explicitly stated otherwise.

II. BASIC PARAMETERS

A. Coupling potential

The relevant coordinates needed to describe the interaction between two Rydberg atoms are $\vec{R}$ (the vector between the two nuclei), $\vec{r}_1$ (the vector between the nucleus of atom 1 and the electron of atom 1), and $\vec{r}_2$ (the vector between the nucleus of atom 2 and the electron of atom 2). We will assume that the nuclei are not close enough for the two electrons to overlap; thus, we do not need to worry about symmetrization of the wave function. The Hamiltonian is

$$H = H_1 + H_2 + V,$$

$$V = \frac{1}{R} - \frac{1}{|\vec{R}+\vec{r}_2|} - \frac{1}{|\vec{R}-\vec{r}_1|} + \frac{1}{|\vec{R}+\vec{r}_2-\vec{r}_1|} \simeq \frac{\vec{r}_1\cdot\vec{r}_2 - 3(\vec{r}_1\cdot\hat{R})(\vec{r}_2\cdot\hat{R})}{R^3}, \quad (1)$$

where H_1 and H_2 are the Hamiltonians for the two Rydberg atoms. In our analysis, we will use only the lowest nonzero coupling potential (dipole-dipole) which is shown above; a more accurate treatment of the potential does not add new physics for the systems that are considered here.

In the next two sections, we give expressions for the matrix elements of the coupling potential between Rydberg states on the two atoms. We will treat the case of Rydberg atoms in zero or weak electric fields separately from the case of atoms in strong, static electric fields. When the atoms are in a weak, static electric field the eigenstates have a well defined angular momentum, while atoms in a strong field have a well defined (large) dipole moment.

1. Field-free case

In the field-free case, we need to evaluate the coupling potential between states of specific angular momentum on different atoms. The matrix elements are effectively evaluated by rewriting the interaction potential in terms of radial and angular pieces. Using angular momentum relationships gives

$$V = -8\pi\sqrt{\frac{2\pi}{15}}\frac{r_1 r_2}{R^3}\sum_{\mu=-2}^{2}[Y_1(\hat{r}_1)Y_1(\hat{r}_2)]^2_\mu Y^*_{2\mu}(\hat{R}), \quad (2)$$

where $[Y_1Y_1]^2_\mu$ means the two spherical harmonics are coupled to total angular momentum 2 and z-component μ through the usual Clebsch-Gordan coefficients.

When there is no electric field, states A and B are eigenstates of angular momentum and have a degeneracy of $2\ell_a+1$ and $2\ell_b+1$. For the case of two atoms interacting through the potential V, there are $2(2\ell_a+1)(2\ell_b+1)$ states of interest: $(2\ell_a+1)(2\ell_b+1)$ when atom 1 is in state A and atom 2 is in state B and $(2\ell_b+1)(2\ell_a+1)$ when atom 1 is in state B and atom 2 is in state A. The only nonzero coupling is between states of type $|AB\rangle$ and $|BA\rangle$. There are no couplings when A,B remain on the same atom due to the $Y_1(\hat{r}_1)$ and $Y_1(\hat{r}_2)$ dependence of the potential. This dependence also means that Rydberg states do not couple unless $|\ell_a-\ell_b|=1$ at this level of approximation of the potential. If the direction between atoms is taken to be in the z direction (i.e., $\hat{R}=\hat{z}$), then m_a+m_b is a conserved quantity.

If we write the Rydberg wave function in the form

$$\psi_{n\ell m}(\vec{r}) = \frac{R_{n\ell}(r)}{r}Y_{\ell m}(\hat{r}) \quad (3)$$

then the matrix element between the states where atom 1 is $n_a\ell_a m_a$, atom 2 is $n_b\ell_b m_b$ and where atom 1 is $n_b\ell_b m'_b$, atom 2 is $n_a\ell_a m'_a$ can be written as

$$V_{AB,A'B'} = -8\pi\sqrt{\frac{2\pi}{15}}\frac{(d_{n_a\ell_a,n_b\ell_b})^2}{R^3}\sum_{\mu=-2}^{2}Y^*_{2\mu}(\hat{R})\langle\ell_a m_a,\ell_b m_b| \times[Y_1(\hat{r}_1)Y_1(\hat{r}_2)]^2_\mu|\ell_b m'_b,\ell_a m'_a\rangle, \quad (4)$$

where the dipole matrix element is defined as

$$d_{n_a\ell_a,n_b\ell_b} = \int_0^\infty rR_{n_a\ell_a}(r)R_{n_b\ell_b}(r)dr. \quad (5)$$

In the special case of the interaction between an s state and a p state, the nonzero matrix elements reduce to

$$V_{1m,00;00,1m'} = -\sqrt{\frac{8\pi}{3}}\frac{(d_{n_a 1,n_b 0})^2}{R^3}(-1)^{m'} \times \begin{pmatrix} 1 & 1 & 2 \\ m & -m' & m'-m \end{pmatrix} Y_{2,m'-m}(\hat{R}), \quad (6)$$

where the $(\cdots)$ is the usual 3-j coefficient.

2. Static electric field

An obvious extension of the previous section is to examine the effect of Rydberg-Rydberg interaction when a strong electric field is in the z direction. A static electric field breaks the spherical symmetry and gives states with substantial dipole moments. This gives a nontrivial difference over the previous section in that there are now nonzero diagonal matrix elements of the coupling potential. Another difference is the large increase in the number of states that can be coupled together through the potential V. The increase in number of states gives rise to interesting physics in the interaction between two Rydberg atoms, but it vastly complicates the study of many atoms. We will examine the full interaction between two Rydberg atoms in a later section. But for the many-atom systems, we will choose two states that couple strongly to each other but weakly to all other states.

The strength of the interaction between Rydberg states can be adjusted by changing their separation. The dipole-dipole interaction, Eq. (1), gives a shift in energy of a pair of Rydberg atoms in Stark states; it also causes a mixing with other Stark states within the n-manifold. If the states A and B are both the highest (or lowest) energy states of the Stark manifold, then the mixing with other pairs of Stark states can be suppressed by increasing the distance between the atoms because no states are degenerate with this pair. For the rest of this section, we will suppress all quantum numbers except the principal quantum number n since the states we are using are specified by being the highest energy state of the Stark manifold. The main important atomic information is the dipole connection between states of different n-manifolds:

$$\langle n|z|n\rangle \simeq \frac{3}{2}n^2,$$

$$\langle n-1|z|n\rangle \simeq \frac{1}{3}n^2,$$

$$\langle n-1|z|n+1\rangle \simeq \frac{1}{9}n^2,$$

$$\langle n|x|n'\rangle = \langle n|y|n'\rangle = 0. \quad (7)$$

Note that the interaction rapidly decreases as the difference in principal quantum number increases. Note also that the x and y part of the interaction has no effect within this approximation. Because the interaction is proportional to the square of the matrix element, we will investigate only the case where the difference in principal quantum number is 1.

For two atoms, the diagonal terms in the interaction are equal and given by

$$V_{n,n';n,n'} = V_{n',n;n',n} = \left(\frac{3nn'}{2}\right)^2 \frac{1-3(\hat{R}\cdot\hat{z})^2}{R^3}. \quad (8)$$

When $|n-n'|=1$, the off-diagonal matrix elements are given by

$$V_{n,n';n',n} = V_{n',n;n,n'} = \left(\frac{nn'}{3}\right)^2 \frac{1-3(\hat{R}\cdot\hat{z})^2}{R^3}. \quad (9)$$

B. Rough estimates

As a check on the feasibility of the experiment proposed below (see Fig. 1), we estimate the effect of processes that were not explicitly included in the model. Also, we estimate the time and distance scales for particular geometries. To get specific numbers, we will use ^{85}Rb ($M=1.4\times10^{-25}$ kg) for the atom. We will also suppose the laser focus size is 3 μm in all dimensions. To keep the situation simple, we look at the case when there are only two atoms in a strong electric field so that the atoms have permanent dipole moments. We assume that the highest energy state of the Stark manifold is excited; the state for atom 1 starts with principal quantum number n_1 and that for atom 2 is n_2. We are interested in the coherent transfer $|n_1 n_2\rangle \rightarrow |n_2 n_1\rangle$.

1. Hopping time scale

The interaction between two atoms in the highest energy Stark state in two different n-manifolds depends on the difference in principal quantum numbers. For a pair of atoms (one in the $n=50$ and the other in the $n=51$ state) separated by 20 μm, the coupling matrix element is 1.3×10^{-11} a.u. when $\hat{R}\cdot\hat{z}\simeq 0$. The time required for the $n=50$ character to hop to the other atom and then back is 2.3×10^{11} a.u. which is 5.7 μs. If the two states are $n=60$ and 61, then the hopping time is reduced to 2.7 μs since the hopping time scales as $1/n^4$. If the distance between the states is reduced to 10 μm, then the hopping time is reduced by a factor of 8 since the time scales as R^3.

2. Atomic motion

The thermal speed $v=\sqrt{3k_BT/M}$ of ^{85}Rb at 300 K is 300 m/s and at 300 μK is 0.3 m/s. The cases we investigate require a few microseconds for interesting effects. Over 1 μs, a Rb atom would travel roughly 1 mm at 300 K and 1 μm at 300 μK. The original region the atom exists in is roughly 3 μm with a separation of 20 μm. Thus, it appears that the atoms would need to be cooled below 1 mK so the states can exchange atoms before they move out of the excitation region. The Heisenberg uncertainty relation does not affect the analysis of the spread of speeds; for a 3 μm spot, the spread in speeds $\Delta v \sim \hbar/(M\Delta x) \sim 2.5\times10^{-4}$ m/s which is much less than the thermal speed at 300 μK.

3. Coherence

We are interested in coherent hopping of the states between atoms. For the hopping to be coherent, the electronic states of the Rydberg atoms cannot couple to other degrees of

freedom. Assuming other particles (e.g., electrons or photons) are not present to contribute decoherence, only the relative motion of the atoms couples to the electronic motion. Previous theoretical studies (see, for example, Ref. [15]) have concluded that the dipole hopping of an excitation through a gas is not coherent unless the temperature is extraordinarily low. In this section we argue that the systems we will investigate are coherent even though the gas is very hot compared to the limit discussed in Ref. [15].

The full wave function for two atoms (with the relative motion of the atoms and the electronic wave functions) can most simply be written as

$$\Psi(t) = \frac{1}{\sqrt{2}}[\psi_+(\vec{R},t)|+\rangle + \psi_-(\vec{R},t)|-\rangle], \tag{10}$$

where the electronic states are defined as

$$|\pm\rangle = \frac{1}{\sqrt{2}}(|AB\rangle \pm |BA\rangle). \tag{11}$$

At the starting time $t=0$, the interatom wave functions are equal: $\psi_+(\vec{R},0)=\psi_-(\vec{R},0)=\psi_0(\vec{R})$. The wave function can be written in terms of the $|AB\rangle$ and $|BA\rangle$ states:

$$\Psi(t) = \frac{1}{2}[\psi_+(\vec{R},t) + \psi_-(\vec{R},t)]|AB\rangle + \frac{1}{2}[\psi_+(\vec{R},t) - \psi_-(\vec{R},t)]|BA\rangle. \tag{12}$$

The probability for finding the atoms with the electronic state $|AB\rangle$ or with the electronic state $|BA\rangle$ without regard for the position of the atoms is

$$P_{AB}(t) = \frac{1}{2}\{1 + \mathrm{Re}[\langle\psi_+(t)|\psi_-(t)\rangle]\},$$

$$P_{BA}(t) = \frac{1}{2}\{1 - \mathrm{Re}[\langle\psi_+(t)|\psi_-(t)\rangle]\}, \tag{13}$$

where we have used the fact that the interatom functions are normalized $\langle\psi_+|\psi_+\rangle=\langle\psi_-|\psi_-\rangle=1$; the symbol Re[ ] means to take the real part of the expression. Clearly, the probabilities have the unitarity property $P_{AB}+P_{BA}=1$. The starting condition gives $P_{AB}=1$ at $t=0$.

The states evolve coherently so long as the + and − functions retain the same form. More specifically, the evolution is coherent only for times where $|\langle\psi_+(t)|\psi_-(t)\rangle|\simeq 1$. To examine this effect we solved the Schrödinger equation for this system. The radial wave functions are the solution of a time-dependent Schrödinger equation

$$i\frac{\partial\,\psi_\pm(\vec{R},t)}{\partial t} = \left[\frac{P^2}{2M} + \left(\frac{3nn'}{2}\right)^2\frac{1-3\,\cos^2\theta}{R^3}\right]\psi_\pm(\vec{R},t) \pm \frac{d^2(1-3\,\cos^2\theta)}{R^3}\psi_\pm(\vec{R},t), \tag{14}$$

where $d=nn'/3$ when $|n-n'|=1$.

The results of this simulation can be understood from simple arguments. The overlap goes to 0 because of the different potentials for the $|+\rangle$ and $|-\rangle$ states. Qualitatively, the two potentials lead to two different forces which cause the packets to move to different positions in space or momentum space. The different forces causes a separation of central position of the ψ_+ and ψ_- wave functions; the difference in the forces is $6d^2/R^4$. The separation after a time t is roughly $\delta x=(\delta F)t^2/2M=3d^2t^2/(MR^4)$. The time required for a complete transition $AB\rightarrow BA\rightarrow AB$ is $T=2\pi/\Delta E=\pi R^3/d^2$. Substituting this in for the time gives $\delta x=3\pi^2R^2/(Md^2)\simeq 1.0\times 10^{-5}(R/d)^2$ Å. For the cases we are thinking about $R/d<10^3$. Thus the positions will separate by less than a nanometer which is much less than the width of the initial wave packet. *No decoherence occurs due to the separation in space of the ψ_+ and ψ_- packets*.

When the atoms do not move far compared to their separation or the localization region, the wave functions are well represented through the impulse approximation

$$\psi_\pm(\vec{R},t) \simeq \exp[-iE_\pm(\vec{R})t]e^{i\phi(\vec{R},t)}\psi_0(\vec{R}), \tag{15}$$

where $\phi(\vec{R},t)$ is a phase common to both wave functions and $E_\pm(\vec{R})=\pm d^2(1-3\,\cos^2\theta)/R^3$ are the relative energies of the ± states if the atoms were fixed with a separation $\vec{R}$. Using this expression to compute the probabilities for finding the atoms in arrangement *AB* or *BA* gives the form

$$P_{AB}(t) = \int P_{AB}(\vec{R},t)P(\vec{R})d^3\vec{R},$$

$$P_{BA}(t) = \int P_{BA}(\vec{R},t)P(\vec{R})d^3\vec{R}, \tag{16}$$

where $P(\vec{R})=|\psi_0(\vec{R})|^2$ is the probability density for finding the atoms with separation $\vec{R}$ and

$$P_{AB}(\vec{R},t) = \frac{1}{2}|e^{-iE_-(\vec{R})t} + e^{-iE_+(\vec{R})t}|^2,$$

$$P_{BA}(\vec{R},t) = \frac{1}{2}|e^{-iE_-(\vec{R})t} - e^{-iE_+(\vec{R})t}|^2 \tag{17}$$

are the probabilities for finding the atoms with the combinations *AB* or *BA* at time t if the atoms are at separation $\vec{R}$. For any specific separation, the probabilities oscillate between 0 and 1 with a frequency proportional to $E_-(\vec{R})-E_+(\vec{R})$. However, the average over $\vec{R}$ in Eq. (16) causes a decoherence due to the spatial dependence of the frequency.

These considerations lead to a simple picture of when the coherence holds. We compute the evolution of the system for many different and random separations $\vec{R}$ that are consistent with an experimental distribution; we average the observables over the different separations. This should be an accurate procedure so long as the conditions are such that the atoms do not move far during the relevant time period.

III. SIMPLE BANDS

A simple case of coherent hopping is when all of the atoms are on a regular lattice. There are many examples of

this type that can be investigated. We chose the simplest example: one p atom with all of the other atoms having s character. We picked a simple geometry (cubic) although others could be equally interesting. Because there are three p states ($m=-1,0,1$), there will only be three bands for each wave number k. Since there is only one p-type atom, the state can be specified by giving the atom that the p state is on and the azimuthal quantum number: $|\beta m\rangle$ will mean that atom β has p character with azimuthal quantum number m and all other atoms are in the s state. To somewhat simplify the notation we will combine parameters:

$$\gamma = \sqrt{\frac{8\pi}{3}}\frac{(d_{n_a 1,n_b 0})^2}{\delta x^3}, \tag{18}$$

where δx is the spacing of the atoms. This parameter has been defined so that the band energy divided by γ is independent of the dipole matrix element and the spacing between atoms.

For a D-dimensional lattice, the eigenstate can be written as the superposition

$$\psi_{\vec{k},\alpha} = \frac{1}{\sqrt{N}}\sum_{\beta' m'} e^{i\vec{k}\cdot\vec{R}_{\beta'}} U_{m'\alpha}(\vec{k})|\beta' m'\rangle, \tag{19}$$

where N is the total number of atoms, $\vec{R}_\beta$ is the position of the β atom, $\vec{k}$ is the wave number, α determines the band at wave number $\vec{k}$, and $U_{m\alpha}(\vec{k})$ is a unitary matrix for any fixed $\vec{k}$. The time-independent Schrödinger equation takes the form

$$H\psi_{\vec{k},\alpha} = \epsilon_\alpha(\vec{k})\psi_{\vec{k},\alpha}. \tag{20}$$

We assume that the diagonal elements of the Hamiltonian have been removed since they are the same for every state. Projecting the state $\langle\beta m|$ onto the Schrödinger equation and using the matrix element from Eq. (6) gives a 3×3 Hermitian diagonalization problem:

$$\sum_{m'} \mathcal{H}_{m,m'}(\vec{k})U_{m',\alpha}(\vec{k}) = U_{m,\alpha}(\vec{k})\epsilon_\alpha(\vec{k}), \tag{21}$$

where the Hermitian matrix is given by

$$\mathcal{H}_{m,m'}(\vec{k}) = -\gamma\delta x^3(-1)^{m'}\begin{pmatrix} 1 & 1 & 2 \\ m & -m' & m'-m \end{pmatrix} \times \sum_{\beta'\neq\beta} e^{-i\vec{k}\cdot\vec{R}_{\beta\beta'}}\frac{Y_{2,m-m'}(\hat{R}_{\beta\beta'})}{R^3_{\beta\beta'}}, \tag{22}$$

where $\vec{R}_{\beta\beta'}=\vec{R}_\beta-\vec{R}_{\beta'}$.

We are interested in the band structure of this system which means the $N\to\infty$ limit. We compute the 3×3 Hermitian matrix by numerical summation, increasing the number of atoms in the sum until convergence is achieved.

The trace of the $\mathcal{H}_{m,m'}$ matrix is 0 for all $\vec{k}$ which constrains the sum of the band energies to be 0. This has the consequence that near $\vec{k}\sim\vec{0}$ there must be bands that have positive effective mass and bands that have negative mass. A wave packet centered at wave number $\vec{k}_0$ has the group velocity for band α:

$$\vec{v}_\alpha(\vec{k}_0) = [\vec{\nabla}_{\vec{k}}\epsilon_\alpha(\vec{k})]_{\vec{k}=\vec{k}_0}. \tag{23}$$

There will be some bands with particle character (positive group velocity proportional to $\vec{k}$ for small $\vec{k}$) and some bands with hole character (negative group velocity proportional to $\vec{k}$ for small $\vec{k}$).

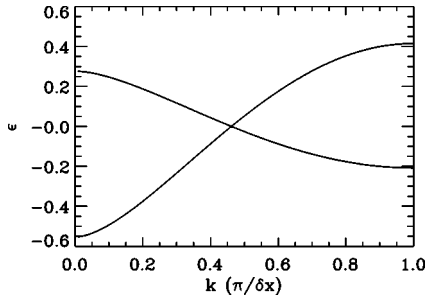

FIG. 2. The scaled band energy [band energy divided by $\sqrt{8\pi/3}(d_{n_a 1,n_b 0})^2/\delta x^3$] as a function of the wave number (in units of $\pi/\delta x$) for a line of atoms with one p state (all other s states). The two bands with the p orbital perpendicular to the line of atoms are degenerate (negative energy near $k=0$). This band structure is very similar to that for an optically excited plasmon wave propagating along metal nanoparticles; see Fig. 1 of Ref. [14]. Note that near $k=0$ some bands have positive curvature (behave like particles with the group velocity the same sign as $\vec{k}$) and some have negative curvature (behave like holes with the group velocity in the opposite direction of $\vec{k}$).

A. Linear lattice

The simplest case is a linear lattice which consists of atoms equally spaced on a line. The band energies are plotted in Fig. 2. Two of the bands are degenerate. These are the bands corresponding to transverse waves (the lobes of the p orbital perpendicular to the line of atoms); the two directions orthogonal to the line of atoms are equivalent. All of the bands have a quadratic k dependence for small k: $\epsilon_\alpha\sim C_\alpha + D_\alpha k^2$. This means the magnitude of the group velocity is proportional to k at small k.

The two degenerate bands have hole character. The band corresponding to the longitudinal wave has particle character. This exactly matches the character of the bands for an optically excited plasmon wave propagating along a series of metal nanoparticles [14]. The degeneracy means that if the bands cross they must cross at $\epsilon=0$. For a perfect lattice, the bands exactly cross because there is no coupling between the longitudinal and transverse waves. If there were defects in the lattice, especially some atoms shifted out of line, then the degeneracy of the two transverse bands would be lifted. Also, the crossing would be replaced by an avoided crossing. If the amount and size of the defects were small, the coupling between the transverse and longitudinal bands would be localized to wave numbers near the avoided crossing.

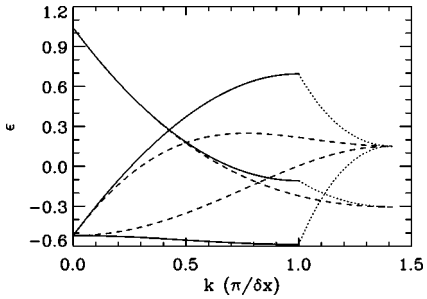

FIG. 3. Same as Fig. 2 but for a square array of atoms. The solid lines are the band energies along the Δ line (center of the Brillouin zone to the center of an edge), the dashed lines are along the Σ line (center of the Brillouin zone to a corner), and the dotted lines are along the *Z* line (center of an edge to an adjacent corner). Two bands (with the lobe of the *p* orbital in the plane of atoms) are degenerate only at the center and a corner of the Brillouin zone. Two of the band energies (the lobe of the *p* orbital perpendicular to $\hat{k}$) are proportional to *k* near $k=0$; excitations of these bands behave more like acoustic phonons or photons (no dispersion). Note some of the bands behave like particles and some like holes near $k=0$. Also, one of the bands (the longitudinal band with the direction of the lobe of the *p* orbital in the same direction as $\vec{k}$) behaves like a hole or a particle depending on the direction (toward the middle of an edge or toward a corner).

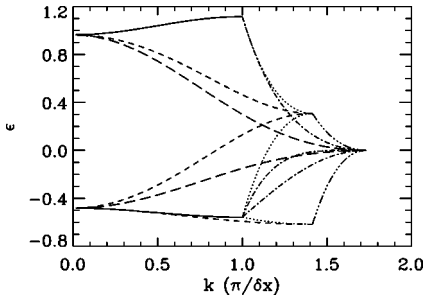

FIG. 4. Same as Figs. 2 and 3 but for a cubic array of atoms. The solid lines are the band energies along the Δ line (center of the Brillouin zone to the center of an edge), the dash-dotted lines are along the *S* line (center of a face to a corner), the dash-dot-dot-dotted lines are along the *T* line (center of an edge to a corner), the short-dashed lines are along the Σ line (center to center of an edge), the dotted lines are along the *Z* line (center of a face to center of an edge), and the long-dashed lines are along the Λ line (center to a corner). As with the two-dimensional example, the bands have particle or hole character near $k=0$ depending on the direction of $\hat{k}$. Note that the corner is a point of triple degeneracy.

B. Square lattice

The bands for a square lattice are two-dimensional functions: $\epsilon_\alpha(k_x,k_y)$. The Brillouin zone for a square lattice has three special points: center $(k_x,k_y)=(0,0)$, which is the Γ point, center of a side $(\pi/\delta x,0)$, which is the *X* point, and the corner $(\pi/\delta x,\pi/\delta x)$, which is the *M* point. A common way of presenting the bands is to plot the band energy along three special lines that connect these points: Δ connects the points Γand *X* (i.e., from the center of the Brillouin zone to the center of a side), Σ connects the points Γ and *M* (i.e., center to corner), and *Z* connects the points *X* and *M* (center of side to corner).

The band energies are plotted in Fig. 3 for these lines as a function of $k=|\vec{k}|=\sqrt{k_x^2+k_y^2}$. The solid lines are the band energies along the Δ line, the dashed lines are along the Σ line, and the dotted lines are along the *Z* line. The character of the eigenvectors lets us assign the different bands. At the center and the corner of the Brillouin zone, two of the bands are degenerate and one is nondegenerate. The nondegenerate band corresponds to the *p* state having $m=0$ character: this is the state whose wave function has a nodal plane in the *xy* plane. Thus, the nondegenerate band has character where the lobes of the *p* state are perpendicular to $\vec{k}$; the band with $m=0$ character crosses the other bands due to the lack of coupling to states with $m=\pm 1$ character. The two degenerate bands at $|k|\to 0$ have the lobes of the *p* state in the *xy* plane. For both the Σ and Δ lines, the band that linearly increases from $|k|=0$ has a *p* state with the lobe perpendicular to $\vec{k}$ while the band that is flat near $|k|=0$ is parallel to $\vec{k}$.

For this system, the bands near $|k|=0$ with *p*-state lobes perpendicular to $\vec{k}$ have band energies that change *linearly* with *k*. These bands have roughly constant group velocity for small $\vec{k}$ and the group velocity does not depend on the direction. Thus the perpendicular bands behave like neither particles nor holes, but like photons or phonons. Interestingly, the nondegenerate band has *negative* group velocity: a wave packet moves in the opposite direction to the wave number. Another interesting feature is that the sign of the group velocity depends on the direction of $\vec{k}$: the longitudinal wave can behave like either a particle or hole depending on $\hat{k}$.

C. Cubic lattice

The Brillouin zone for a cubic lattice has four special points: center $(k_x,k_y,k_z)=(0,0,0)$, which is the Γ point, center of a face $(\pi/\delta x,0,0)$, which is the *X* point, center of an edge $(\pi/\delta x,\pi/\delta x,0)$ which is the *M* point, and a corner $(\pi/\delta x,\pi/\delta x,\pi/\delta x)$, which is the *R* point. We have computed the bands along six lines that connect these points: Δ connects Γ and *X* (center of the Brillouin zone to the center of a face), *S* connects *X* and *R* (center of a face to a corner), *T* connects *M* and *R* (center of an edge to a corner), Σ connects Γ and *M* (center to center of an edge), *Z* connects *X* and *M* (center of a face to center of an edge), and Λ connects Γ and *R* (center to a corner).

The band energies are plotted in Fig. 4 for these lines as a function of $k=|\vec{k}|=\sqrt{k_x^2+k_y^2+k_z^2}$. The character of the eigenvectors lets us assign the different bands. All four of the special points have degenerate states and the Δ, *T*, and Λ lines have degenerate bands. The two bands with the *p* state perpendicular to $\hat{k}$ are degenerate at the Γ, *X*, and *M* points and *all* states are degenerate at the *R* point (corner). For the Δ, *T*, and Λ lines the two bands with the *p* state perpendicular to $\hat{k}$ are degenerate; for Δ and Λ these are the lower energy bands while the degenerate bands are the higher energy bands for *T*.

The bands show a remarkable richness for such a simple system. All of the bands near $k\sim 0$ have particle or hole character depending on the direction of $\hat{k}$. But, interestingly, whether a band has particle or hole character near $k=0$ depends on the direction of $\vec{k}$. The cubic lattice is also interesting because the interaction is *not* well approximated by only including nearest neighbor (or even next nearest neighbor) interactions. Because the number of atoms in a spherical shell increases proportional to R^2 while the interaction decreases like $1/R^3$, the atoms at large distances must be included for accurate band energies near $k\sim 0$. The sum in Eq. (22) only converges due to the presence of the $Y_{2\mu}(\hat{R})$ and the $\exp(i\vec{k}\cdot\vec{R})$; the changing signs of these functions give cancellations that converge the sum. The $k=0$ limits can be found analytically by converting the sum in Eq. (22) into an integral; the integral can be performed analytically which gives the energy of the band with the p state parallel to $\hat{k}$ as $\epsilon=\sqrt{8\pi/27\gamma}$ and the energies of the degenerate perpendicular states at $\epsilon=-\sqrt{2\pi/27\gamma}$.

IV. AMORPHOUS DISTRIBUTION

In Refs. [2–6], a cold gas is excited to Rydberg states that can make degenerate transitions to nearby states. A typical description of this system is that a state hops away after making the transition. We have investigated the hopping assumption through large numerical diagonalization. Our results are not in complete agreement with previous theoretical investigations [4,5] but do support the main conclusions.

We performed calculations with two models. In both models, a single p-type atom is in a gas of s-type atoms. The N atoms are randomly positioned within a cube with a length L so that the density is N/L^3; to minimize the effect of the surfaces, we use a cyclic interaction between the atoms: the x difference is ΔX_{ij} which is given by whichever is smaller in magnitude X_i-X_j or $X_i-X_j\pm L$ (with a similar prescription for the y and z components). For a given number of atoms, we performed M independent calculations with the atoms at random positions. We increased N until convergence was achieved.

In the first model, we used the form of the interaction that was used in previous studies [4,5]. This is a simplified form of the dipole-dipole interaction where only the radial dependence of the interaction is retained. Defining the state $|j\rangle$ to be the atom with p character, a scaled interaction Hamiltonian is defined as

$$\overline{H}_{ij}=\frac{1}{N}\left(\frac{L}{|\Delta\vec{R}_{ij}|}\right)^3 \tag{24}$$

for $i\neq j$ and $\overline{H}_{ii}=0$. The main simplification in this Hamiltonian is the fact that the coupling is the same sign with every atom and the degeneracy of the p state is ignored. The scaling removes the trivial dependence on the dipole strengths and the density.

In the second model, we used the form of the interaction in Eq. (6). This is a somewhat more realistic interaction since it accounts for the angular momentum of the Rydberg electron; however, in the actual experiments, the states are eigenstates of the *total angular momentum* of the Rydberg electron (spin plus orbital) which changes the details of the interaction. Because we include the degeneracy of the p states in this model, the number of states is $3\times$ the number of atoms. Again, we have scaled the interaction potential to remove the trivial dependence on the density and the dipole strengths:

$$\overline{H}_{ij}=V(\Delta\vec{R}_{ij})\frac{L^3}{d^2N}. \tag{25}$$

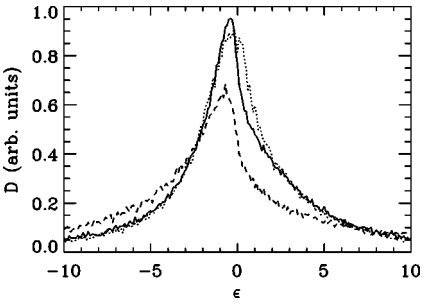

FIG. 5. The distribution of energies for a random placement of Rydberg atoms: N Rydberg atoms are randomly positioned within a cube and cyclic approximation is used for the interaction potential. The energies are scaled as discussed in the text. The solid line and dotted line are for one p state and $N-1$ s states: the solid line is the average of many geometries with $N=216$ and the dotted line is the average of many geometries with $N=8$. This suggests that (except for the small region $-1<\epsilon<1$) the main determination of the energy depends on fewer than eight atoms. The dashed line is for the simplified interaction potential used in previous theoretical treatments; this potential simplifies the angular dependence of the interaction.

In Fig. 5, we show the distribution of eigenenergies for the two models. We obtained the distribution by diagonalizing the interaction Hamiltonian for random placement of N atoms within a cube with a cyclic approximation to the interaction. We averaged over a sufficient number of independent geometries to obtain a smooth curve. Finally, we increased the number of atoms in a single geometry until the distribution was independent of the number of atoms. The distributions for the simplified model and more realistic model give qualitatively similar results, but there are differences. The more realistic model has a somewhat narrower distribution which means that the simplified model will tend to give faster hopping. The qualitatively similar shapes of the two models reflect the radial dependence of the strength and the random placement of the atoms.

In Fig. 6, we show the time dependence of the probability for finding the p state at the atom it started on. It is clear from this figure that the more simplified interaction, Eq. (24), substantially differs from the interaction that includes the correct effect from the angular momenta and the angular dependence in V. However, the difference between the models is quantitative and the main conclusions from previous theories seem to be unchanged. It is interesting that most of the dependence in both figures is already present with eight atoms; this is because the p state is distributed over few atoms

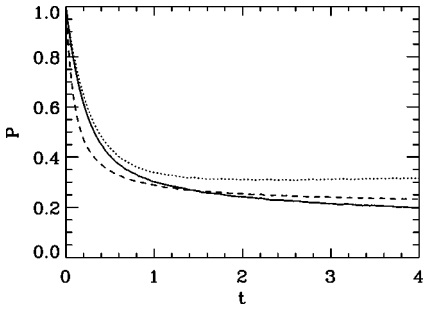

FIG. 6. The probability P for finding the p state on the same atom that it starts on as a function of scaled time. The line types are the same as in Fig. 5. Note that the fast drop in probability is well reproduced with eight atoms, which shows that most of the drop is due to hopping to adjacent atoms. The longer time development shows the hopping of the p state further from its original position.

at short times. For the energy distribution, there is only a small energy range (width roughly 1 in scaled units) that changes with the number of atoms. For the time-dependent probability in Fig. 6, the rapid drop (to roughly $P=1/2$) is accurately reproduced with eight atoms. It is the slower decay (and small energies) that depends on the number of atoms. Note that the probability for the excitation to remain on the starting atom does not decrease to 1 divided by the number of atoms but is much higher: roughly between $1/6$ and $1/4$.

This scenario can be explained because the large energy shifts and the corresponding rapid drop in time are due to close pairs which give large interactions H_{ij}. Close pairs roughly act like isolated systems because the pair energy shifts them out of resonance with the rest of the atoms; this is similar to the dipole blockade idea [13]. The p state then hops back and forth between the close atoms; it is pinned to the defect at early times. However, there are some regions within the gas where many atoms are roughly equidistant; within these regions the p state can diffuse far from the initial atom.

This idea can be quantified. If $P_{j,j_0}(t)$ is the probability that the p state is on atom j when it starts on state j_0, then the quantity $\mathcal{N}\equiv[\Sigma_j P_{j,j_0}^2(t)]^{-1}$ roughly tracks the number of atoms the p state is spread over if it starts on atom j_0. For the more sophisticated model, there are geometries and j_0 that did not allow the p state to spread (roughly 24% starting j_0 spread over four or fewer atoms at $t=4$).The remaining part of the population was spread over a wide distribution of atoms which seems to represent the p state hopping away from the original atom.

V. HOPPING IN A SMALL NONPERFECT LATTICE

The hopping of a Rydberg excitation between atoms has been invoked to explain the results in Refs. [2–6]. We note that this hopping could be directly measured. This can be accomplished by having a laser excite small regions of a gas into a Rydberg state A; a second laser can excite a disjoint region into a state B. By using a CCD camera and state selective field ionization, the character of the Rydberg state in each region can be ascertained and the hopping of the Rydberg state can be seen experimentally.

Since we imagine the states will be distinguished by ramping an electric field, we will assume the atoms are always in a strong electric field and that the Rydberg states are Stark states. The interaction between the Rydberg states will be through Eqs. (8) and (9). To be specific, we will treat the case where one atom is excited to the $n=61$ state and all other atoms are in $n=60$. Each Rydberg atom is created randomly within a cube with edge length of 3 μm and nearest neighbor separation of 20 μm. For all cases, we imagine the electric field is perpendicular to the line or plane of atoms so $\hat{z}\cdot\hat{R}\sim 0$.

We plot the results for a line of atoms in Fig. 7; for all cases, the regions are along the x-axis with the $n=61$ state starting in the leftmost region. The simplest result is when there are only two atoms, Fig. 7(a). The probability for finding the $n=61$ state in the leftmost region is plotted as the solid line and the probability for finding the $n=61$ state in the rightmost region is the dotted line. If we were to pick a specific distance between the atoms, the probability would oscillate between 0 and 1 like $\cos^2\omega t$. Because the distribution is somewhat random in space, there is a range of frequencies that need to be averaged over and this gives the damping. The next case we plot, Fig. 7(b), is for six atoms: one atom of $n=61$ and five of $n=60$. Again we started the $n=61$ state in the leftmost region. The solid line shows the probability for finding the $n=61$ state in the leftmost region, the dotted line is for finding it in the region adjacent to the starting region, and the dashed line shows the probability for finding it in the rightmost region. It is interesting that the probability for finding the $n=61$ state in the region adjacent to the starting region peaks just after it leaves the leftmost region and just before it reenters the leftmost region. It is somewhat surprising that the probability for finding $n=61$ in the leftmost region recurs up to 0.3 at ~ 8 μs since the two-atom case has damped to the average value by that time. Note also that the probability for finding $n=61$ in the rightmost region peaks at ~ 4 μs to a value of 0.3. The probabilities oscillate out to ~ 20 μs and shows that the coherence survives the spatial averaging for substantial times. For the last case, Fig. 7(c), we show the effect of having an atom missing from one of the regions; this case has five atoms in six regions with the pattern 61,60,skip,60,60,60 (i.e., there is no Rydberg atom in the third region). The solid curve is the probability for finding the $n=61$ state in the leftmost region, the dotted curve is the probability for being in the adjacent region, and the dashed curve is the probability for finding it past the skipped region. The probability for finding $n=61$ in the two leftmost regions behaves as in the two-atom case, Fig. 7(a), and there is very little probability for finding it beyond the skip region during the first 10 μs. The $n=61$ state has a difficult time jumping the gap caused by the missing atom because the interaction between region 2 and region 4 is a factor of 8 smaller than that between successive regions. A similar effect occurs if there are two atoms within the same region; the two nearby atoms interact so strongly that the pair energy is well shifted away from the band energy so they do not interact strongly with the rest of the atoms.

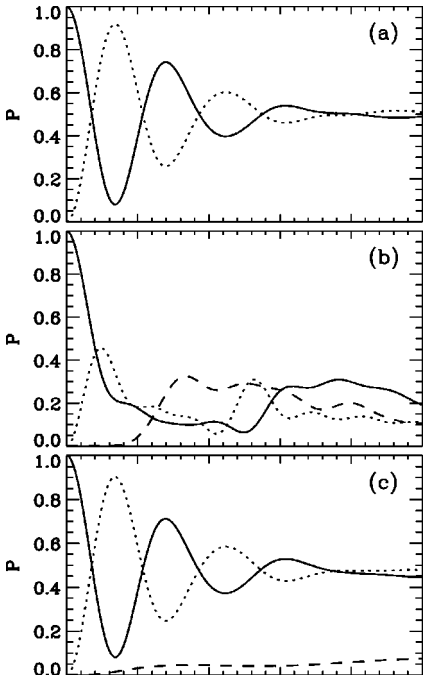

FIG. 7. The probability P for finding the $n=61$ state on various atoms. Atoms are excited within regions that are separated by 20 μm and each of the regions has a width of 3 μm as drawn in Fig. 1. (a) For two regions, the probability for finding the $n=61$ state in the leftmost region is plotted as the solid line and the probability for finding the $n=61$ state in the rightmost region is the dotted line. (b) There are six atoms: one atom of $n=61$ and five of $n=60$. Again we started the $n=61$ state in the leftmost region. The solid line shows the probability for finding the $n=61$ state in the leftmost region, the dotted line for finding the $n=61$ in the region adjacent to the starting region, and the dashed line shows the probability for finding it in the rightmost region. (c) We show the effect of having an atom missing from one of the regions; this case has five atoms in six regions with the pattern 61,60,skip,60,60,60 (i.e., there is no Rydberg atom in the third region). The solid curve is the probability for finding the $n=61$ in the leftmost region, the dotted line is for finding it adjacent to the starting region, and the dashed line is for finding it in any of the three regions past the skip. The probability for finding $n=61$ in the leftmost regions behaves as in the two-atom case (a) and there is very little probability for finding it beyond the skip region during the first 10 μs. The skipped region blocks the hopping.

These are not the only interesting cases of Rydberg atoms in a line. We have investigated several other cases (atoms arranged in a circle geometry, four atoms in the pattern 61,60,skip,60,60, N atoms in the pattern 61,skip,60,60,60,60,…, two atoms in the excited state 61,60,60,60,61, etc.). Each of these has features that would be worth more detailed studies.

We plot the results for a two-dimensional array of atoms in Fig. 8. Again, we investigated several cases but present results for only one of them. This case is a 2×2 grid of atoms. The solid line is the probability for finding the $n=61$ state on the atom it started on, the dotted line is the probability for finding it on either of the atoms in adjacent corners, and the dashed line is the probability for finding it on the opposite corner. We note that the $n=61$ state seems to first jump to the adjacent corner before jumping to the opposite corner. We find that the coherence is somewhat less sensitive to the randomness in the relative positions of the atoms for the square lattice; this means we could reduce the distance between atoms and preserve coherence.

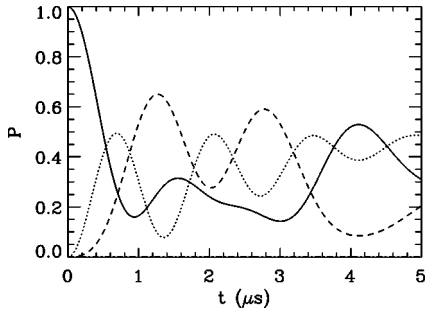

FIG. 8. The probability for finding the $n=61$ state on different atoms for a 2×2 grid of atoms. The solid line is the probability for finding the $n=61$ state at the atom it started on, the dotted line is the probability for finding it on either of the atoms in adjacent corners, and the dashed line is the probability for finding it on the opposite corner. Note the probability for finding the $n=61$ state at an adjacent corner peaks before finding it at the opposite corner; this indicates the excitation hops to the nearby atoms then to the opposite corner.

VI. STRONG RYDBERG-RYDBERG INTERACTION

An essential states model has been assumed in previous treatments of Rydberg-Rydberg interactions. We investigate the validity of this assumption. In the next section, we numerically solve the time-dependent Schrödinger equation for a model interaction between atoms. With this model, we investigate when the Rydberg atoms will make transitions to n-states outside of those being explicitly treated. In the following section, we numerically solve for the interaction between two hydrogen atoms where transitions can be made within the n-manifold. This investigation also affects the predictions of Ref. [12] where the interaction between two Stark states (approximated by an essential states model) was an important aspect of using the dipole-dipole interaction for "fast quantum gates." As shown below, the essential states model is only accurate for a strong enough electric field; the strength depends on the distance between the atoms and should be achievable.

A. n-changing interaction

We solve the time-dependent Schrödinger equation for the model potential $V(r_1,r_2)=-1/r_1-1/r_2+r_1r_2/R^3$. The limit $R\rightarrow\infty$ gives two isolated atoms. The atoms have outer radial turning points at $r_1=2n_1^2$ and $r_2=2n_2^2$. We examined two cases: (1) when $n_1=n_2=n$ and (2) when $n_1=n, n_2=n+1$. Within the essential states model, the first case is nondegenerate; however, we note that the states with $n_1=n+1, n_2=n-1$ and $n_1=n-1, n_2=n+1$ are shifted in energy by $3/n^4$ from the initial state, $n_1=n_2=n$. In case 2, this state is degenerate with $n_1=n+1, n_2=n$ but again there are states that differ by energies of order $1/n^4$. The results for the limitations of the

essential states model was similar for both initial states. We report the details for model 1 where both atoms start in the same n-state.

We expanded the wave function in a basis of states $\psi_{n_1}(r_1)\psi_{n_2}(r_2)$ and increased the number of basis functions until convergence was achieved. The basis set consisted of all pairs of functions with n_1 and n_2 between $n-\Delta n$ and $n+\Delta n$; we increased Δn until the time-dependent wave function was converged. We started with the distance between the atoms at $R=8n^2$ and reduced R until the initial state started to substantially mix. The states n,n are most strongly coupled to $n-1,n+1$ and $n+1,n-1$ due to the small energy difference: $|\varepsilon_n+\varepsilon_n-\varepsilon_{n-1}-\varepsilon_{n+1}|\sim 3/n^4$. We computed the probability of finding the pair of atoms in the three states n,n and $n\mp 1,n\pm 1$ when the atom started in the state n,n. We found that the probability for finding the atom pair in these states decreased to $\sim$90% at $R\sim 8n^2$ for $n=40$ and the probability decreased to $\sim$50% at $R\sim 4.5n^2$ for $n=40$ and $R\sim 5.2n^2$ for $n=60$.

Our conclusion is that the transition between n-manifolds should be weak for $R>10n^2$ as long as $n<80$ unless accidental degeneracies are present. This distance is somewhat smaller than might be expected. The important point is that the transition matrix element $n,n\rightarrow n-1,n+1$ or $n+1,n-1$ is proportional to $(n^2/3)^2$ since there are two dipoles between states in different n-manifolds; the $(1/3)^2$ reduces the coupling by an order of magnitude over what might be expected. For different applications that require the mixing to be less than 10% the distance would need to be larger. Using these values, we find that the distance at which the essential states approximation becomes problematic is $R\sim 2$ μm for $n=60$ which is much smaller than the values used in the simulations of the previous section.

B. Within Stark manifolds

The interaction between two H atoms in an electric field F gives rise to a potential

$$V=(z_1+z_2)F+\frac{1}{R^3}[\vec{r}_1\cdot\vec{r}_2-3(\vec{r}_1\cdot\hat{R})(\vec{r}_2\cdot\hat{R})], \tag{26}$$

which gives the Stark splitting of the energy levels and couples together the states within the n-manifolds. For the special case of two H atoms, we can compute the matrix elements between the different states using the usual decomposition of the $\vec{r}$ operators in terms of the scaled Runge-Lenz vector [16]:

$$\vec{r}_1=\frac{3}{2}n_1\vec{A}_1,\quad \vec{r}_2=\frac{3}{2}n_2\vec{A}_2. \tag{27}$$

The scaled Runge-Lenz vector and the orbital angular momentum operators can be expressed in terms of commuting angular momenta

$$\vec{L}_1=\vec{J}_1+\vec{J}_2,\quad \vec{A}_1=\vec{J}_1-\vec{J}_2,$$

$$\vec{L}_2=\vec{J}_3+\vec{J}_4,\quad \vec{A}_2=\vec{J}_3-\vec{J}_4. \tag{28}$$

Although many aspects of H atoms in fields have been explored, we do not know of any treatments of a pair of interacting H atoms at this level of approximation. This model should be the subject of a more detailed study than that presented in this section.

For a single atom in a static electric field, the projection of Stark states on angular momentum states is simply the Clebsch-Gordan coefficients since $\vec{L}$ is the addition of the two angular momenta

$$\langle\psi_{n\ell m}|\psi_{nj_1m_1j_2m_2}\rangle=\langle\ell m|j_1m_1j_2m_2\rangle. \tag{29}$$

The magnitude of $\vec{J}_1$ and $\vec{J}_2$ are both $j_1=j_2=(n_1-1)/2$. The range of the azimuthal quantum number is $-j_1\leqslant m_1\leqslant j_1$. The change in the energy due to the electric field is $E_{m_1m_2}=3Fn_1(m_1-m_2)/2$. The maximum energy is when $m_1=j_1=(n_1-1)/2$ and $m_2=-j_2=-(n_1-1)/2$.

In terms of the commuting angular momenta, the coupling potential can be written as

$$V=\frac{3}{2}F[n_1(J_{1z}-J_{2z})+n_2(J_{3z}-J_{4z})]+\frac{9n_1n_2}{4R^3}\times\{(\vec{J}_1-\vec{J}_2)\cdot(\vec{J}_3-\vec{J}_4)-3[(\vec{J}_1-\vec{J}_2)\cdot\hat{R}][(\vec{J}_3-\vec{J}_4)\cdot\hat{R}]\}. \tag{30}$$

The eigenstates of this interaction will be a superposition of the states which we write as $|m_1,m_2,m_3,m_4\rangle$ (for notational simplicity we suppress the j and n quantum numbers since they are fixed for specified n-manifolds). The highest energy state when $R\rightarrow\infty$ is $|j_1,-j_2,j_3,-j_4\rangle$ which corresponds to both atoms being in the highest energy state of the Stark manifold.

The dipole-dipole interaction acts to mix the Stark states. The mixing can be suppressed if the spacing between the Stark states is large compared to the coupling matrix elements. We examined two special cases ($\vec{R}$ parallel to $\vec{F}$ and $\vec{R}$ perpendicular to $\vec{F}$) to determine the distance R where the Stark states start becoming mixed for a fixed external field F. We found that the transition from little mixing to complete mixing occurred over a small region of R. The separation distance between strong mixing and little mixing is roughly the distance where the dipole electric field from one atom is comparable to the external field: $n^2/R^3\sim F$. This implies the atoms will need a distance greater than $R_{cut}\sim Cn^{2/3}F^{-1/3}$ for the essential states approximation to hold; the parameter C is independent of n and F. If F is in V/cm and R is in μm then calculations for $n=41$, 61, 81 give $C\sim 0.16$ when $\hat{R}=\hat{z}$.

However, it is important to note that if F is too large then states between different n-manifolds start mixing and then further complications arise from jumps to adjacent n-manifolds. The n-mixing field strength is $F\simeq 1/(3n^5)$. The minimum distance that allows the essential states approximation will be when the field is slightly less than $1/(3n^5)$; this

field gives the minimum $R_{cut} \sim Dn^{7/3}$ where $D \sim 1.35 \times 10^{-4}$ μm when $\hat{R} = \hat{z}$; D is reduced slightly to 1.1×10^{-4} μm when $\hat{R} = \hat{x}$. It is important to note that the minimum distance where the essential states approximation works well increases faster than the size of the atom which increases as n^2.

For the $n = 60$ state, the minimum distance for which the essential states model works is roughly 2 μm. Thus, the essential states model should be a very good approximation for the examples described in previous sections.

VII. CONCLUSIONS

We have investigated several aspects of strong interactions in a Rydberg gas. We performed a full simulation of the motion of two atoms to obtain the conditions when the interaction between Rydberg atoms is coherent; in contradiction with previous studies, we expect the dipole hopping of Rydberg excitations to be coherent. We also investigated the limitations of the essential states model since this has been the foundation of previous treatments of both Rydberg gases and effects such as the dipole blockade; we introduced two models (which could be investigated more deeply) to study the transitions to adjacent n-manifolds and transitions within an n-manifold.

We investigated the hopping of an excitation through a Rydberg gas in various configurations. We studied two models with random placement of atoms and found that the main points of previous discussions of this situation [2–6] were correct although more realistic models affect the quantitative properties. We studied the band structure for a perfect lattice of Rydberg atoms and found many similarities with studies of optical excitations along metal nanoparticles. We also studied small arrays of atoms in nearly regular arrangements since these are more experimentally accessible. We found that the Rydberg excitation should coherently hop between atoms in configurations that are experimentally accessible.

ACKNOWLEDGMENTS

We gratefully acknowledge conversations with T. F. Gallagher. This work was supported in part by the NSF and in part by the research program of the Stichting voor Fundamenteel Onderzoek der Materie (FOM), which is financially supported by the Nederlandse Organisatie voor Wetenschappelijk Onderzoek (NWO).

[1] K. A. Safinya, J. F. Delpech, F. Gounand, W. Sandner, and T. F. Gallagher, Phys. Rev. Lett. **47**, 405 (1981).
[2] W. R. Anderson, J. R. Veale, and T. F. Gallagher, Phys. Rev. Lett. **80**, 249 (1998).
[3] I. Mourachko, D. Comparat, F. de Tomasi, A. Fioretti, P. Nosbaum, V. M. Akulin, and P. Pillet, Phys. Rev. Lett. **80**, 253 (1998).
[4] V. M. Akulin, F. de Tomasi, I. Mourachko, and P. Pillet, Physica D **131**, 125 (1999).
[5] J. S. Frasier, V. Celli, and T. Blum, Phys. Rev. A **59**, 4358 (1999).
[6] W. R. Anderson, M. P. Robinson, J. D. D. Martin, and T. F. Gallagher, Phys. Rev. A **65**, 063404 (2002).
[7] J. M. Raimond, G. Vitrant, and S. Haroche, J. Phys. B **14**, L655 (1981).
[8] A. Fioretti, D. Comparat, C. Drag, T. F. Gallagher, and P. Pillet, Phys. Rev. Lett. **82**, 1839 (1999).
[9] R. A. D. S. Zanon, K. M. F. Magalhaes, A. L. de Oliveira, and L. G. Marcassa, Phys. Rev. A **65**, 023405 (2002).
[10] A. L. de Oliveira, M. W. Mancini, V. S. Bagnato, and L. G. Marcassa, Phys. Rev. Lett. **90**, 143002 (2003).
[11] S. M. Farooqi, D. Tong, S. Krishnan, J. Stanojevic, Y. P. Zhang, J. R. Ensher, A. S. Estrin, C. Boisseau, R. Cote, E. E. Eyler, and P. L. Gould, Phys. Rev. Lett. **91**, 183002 (2003).
[12] D. Jaksch, J. I. Cirac, P. Zoller, S. L. Rolston, R. Coté, and M. D. Lukin, Phys. Rev. Lett. **85**, 2208 (2000).
[13] M. D. Lukin, M. Fleischhauer, R. Coté, L. M. Duan,D. Jaksch, J. I. Cirac, and P. Zoller, Phys. Rev. Lett. **87**, 037901 (2001).
[14] S. A. Maier, P. G. Kik, and H. A. Atwater, Phys. Rev. B **67**, 205402 (2003).
[15] B. V. Svistunov and G. V. Shlyapnikov, Sov. Phys. JETP **70**, 460 (1990).
[16] E. Merzbacher, *Quantum Mechanics*, 3rd ed. (John Wiley and Sons, New York, 1998).